View metadata, citation and similar papers at core.ac.uk

brought to you by CORE

provided by NASA Technical Reports Server

General Disclaimer

One or more of the Following Statements may affect this Document

- This document has been reproduced from the best copy furnished by the organizational source. It is being released in the interest of making available as much information as possible.

- This document may contain data, which exceeds the sheet parameters. It was furnished in this condition by the organizational source and is the best copy available.

- This document may contain tone-on-tone or color graphs, charts and/or pictures, which have been reproduced in black and white.

- This document is paginated as submitted by the original source.

- Portions of this document are not fully legible due to the historical nature of some of the material. However, it is the best reproduction available from the original submission.

Produced by the NASA Center for Aerospace Information (CASI)

NASA CR 137632

Department of Aerospace Engineering
University of Cincinnati

FLOW BEHAVIOR IN INLET GUIDE VANES OF RADIAL TURBINES

BY

J. SOKHEY, W. TABAKOFF AND W. HOSNY

(NASA-CR-137632) FLOW BEHAVIOR IN INLET GUIDE VANES OF RADIAL TURBINES (Cincinnati Univ.) 33 p HC $4.00 CSCL 20D

N76-17029

Unclas
G3/02 13652

NASA STI FACILITY
INPUT BRANCH

Supported by:

NATIONAL AERONAUTICS AND SPACE ADMINISTRATION

Ames Research Center

Contract No. NAS2-7850

NASA CR 137632

FLOW BEHAVIOR IN INLET GUIDE VANES OF RADIAL TURBINES

by

J. Sokhey, W. Tabakoff and W. Hosny

Supported by:

NATIONAL AERONAUTICS AND SPACE ADMINISTRATION

Ames Research Center

Contract No. NAS2-7850

1. Report No NASA CR 137632	2. Government Accession No.	3. Recipient's Catalog No.
4. Title and Subtitle Flow Behavior in Inlet Guide Vanes of Radial Turbines		5. Report Date October 1975 6. Performing Organization Code
7. Author(s) J. Sokhey, W. Tabakoff and W. Hosny		8. Performing Organization Report No. 10. Work Unit No.
9. Performing Organization Name and Address Department of Aerospace Engineering University of Cincinnati Cincinnati, Ohio 45221		11. Contract or Grant No. NAS2-7850
12. Sponsoring Agency Name and Address National Aeronautics and Space Administration Washington, D.C. 20546		13. Type of Report and Period Covered Contractor Report 14. Sponsoring Agency Code

15. Supplementary Notes

Project Manager, Major G. Godfrey, U.S. Army Air Mobility Research and Development Laboratory, Ames Research Center, Moffett Field, California 94035

16. Abstract

A brief discussion on the scroll flow is presented. Streamline pattern and velocity distribution in the guide vanes are calculated. The blade surface temperature distribution is also determined. The effects of the blade shapes and the nozzle channel width on the velocity profiles at inlet to the guide vanes are investigated.

17. Key Words (Suggested by Author(s))	18. Distribution Statement
Radial Turbine Scroll Guide Vane	Unclassified - unlimited

19. Security Classif. (of this report)	20. Security Classif. (of this page)	21. No. of Pages	22. Price*
Unclassified	Unclassified	32	

* For sale by the National Technical Information Service, Springfield, Virginia 22151

TABLE OF CONTENTS

SUMMARY

A brief discussion on the scroll flow is presented. Streamline pattern and velocity distribution in the guide vanes are calculated. The blade surface temperature distribution is also determined. The effects of the blade shapes and the nozzle channel width on the velocity profiles at inlet to the guide vanes are investigated.

INTRODUCTION

In recent years there have been considerable developments in the study of small radial gas turbines to improve their performance characteristics (References 1 through 3). Most of this research work has been concentrated on turbine rotors, since it was considered to have the main effect on turbine efficiency. Recent experimental works have shown the need for new design techniques in the turbine scroll and guide vanes in order to improve the turbine performance.

At the present time the scroll designs are still based on one dimensional flow calculations. Guide vane blades are merely designed to give the required flow turning angle. The inlet velocity distribution has been assumed to be uniform from one guide vane to another. Such an assumption is not realistic; a variation in the inlet velocity distribution exists and depends mainly on the scroll and the guide vane blade effects. The scroll effects on inlet velocity profiles are discussed in this report, but no final solution is given. The analysis presented here deals only with the guide vane blade effects on the variation in the inlet velocity profiles.

SCROLL EFFECT ON GUIDE VANE INLET VELOCITY VARIATIO!

The three dimensional flow behavior in the scroll affects the nozzle inlet flow properties. A circumferential variation in the flow properties and lateral velocity components result from the secondary flow discharge effects in the scroll.

Boundary layer build-up on scroll side walls has a blocking effect in the scroll passage. Consequently, each vane will have different inlet conditions, especially the inlet mass flow and the inlet flow incidence.

The secondary flow in the scroll results from the non-equilibrium between the pressure and the centrifugal forces in the boundary layers on the scroll side walls. Nonuniformities in the flow properties at the scroll inlet also result in secondary flow. This effect is similar to the secondary flow in cascade passages and pipe bends (References 4 and 5). The

secondary flow consists mainly of a pair of vortices, as shown in Figure 1. Their strength increases along the scroll, causing a circumferential variation in the flow parameters. This is another factor that leads to different inlet flow condition in each guide vane channel.

Additional weak vortices are created in the scroll passage due to the flow discharge to the guide vanes. Such vortices are similar to the corner vortices, but are not stationary. These vortices depend on the geometry of the scroll and nozzle entrance arrangements. Two discharge vortices are created when the vane entrance is at the middle of the scroll cross section. However, only one vortex is induced when the vane entrance is at the scroll side, as shown in Figure 2. Lateral velocity components will result at the guide vane entrance due to the secondary flow and the discharge effects in the scroll.

GUIDE VANE BLADE EFFECT ON INLET VELOCITY DISTRIBUTION AND FLOW CHARACTERISTICS IN THE NOZZLE

The flow in the stagnation regions is largely affected by the vane blades leading edge geometry and by their setting. This in turn strongly influences the flow at the vane channel inlet. The effects of these geometry parameters, as well as the passage depth shape in the axial direction on the inlet velocity profile are considered in the present work.

The mass flow distribution between the guide vane nozzles is assumed to be known from the scroll data. The flow properties are taken to be uniform at the scroll exit, and the variation in the flow properties occurs when the flow passes through the nozzle entrance region. The nozzle entrance is considered to be the part which connects the scroll exit with the guide vane, i.e., the region between stations 2 and 3 of Figure 3. The entrance region radial length is usually about half the guide vane blade radial chord. If we assume a uniform flow away from the guided vane blades, Katsanis' program (Reference 6) for calculating velocities on a blade-to-blade stream surface of a turbomachine could be used to study the

flow field and determine the profiles at station 3. A brief review of the analysis used in this computer program follows.

There are two useful techniques for calculating velocities through radial cascades; namely the velocity gradient method and the finite difference method. Advantages of both methods are utilized in the analysis.

The stream function equation for the radial guide vane cascades is given by

$$\frac{1}{r^2}\frac{\partial^2\chi}{\partial\theta^2} + \frac{\partial^2\chi}{\partial r^2} - \frac{1}{r^2}\frac{1}{\rho}\frac{\partial\rho}{\partial\theta}\frac{\partial\chi}{\partial\theta} - \left(\frac{1}{r} + \frac{1}{b\rho}\frac{\partial(b\rho)}{\partial r}\right)\frac{\partial\chi}{\partial r} = 0 \qquad (1)$$

where χ is a stream function which satisfies

$$\frac{\partial\chi}{\partial r} = \frac{b\rho}{w} W_\theta \quad , \quad \frac{\partial\chi}{\partial\theta} = -\frac{b\rho}{w} W_r \qquad (2)$$

where w is nozzle vane mass flow
W_r, W_θ are velocity components.

Finite difference techniques are used to solve the stream function in the finite region ABCDEFGH as shown in Figure 4. The flow at a radial distance ℓ, from the guide vane blades, is assumed to be uniform with a constant flow angle α, measured from the radial direction.

When the local velocities inside the region are supersonic, then equation (1) is no longer elliptic and a different technique has to be used. For such a case, a different approach is followed which is based on velocity gradient method. The velocity gradient equations were derived in Reference 6. For our radial cascade they can be written as follows:

$$\frac{\partial W}{\partial\theta} = AW + B \qquad (3)$$

where

$$A = \sin^2\beta\left\{2\,\frac{\frac{\partial^2\chi}{\partial\theta\partial r}}{\frac{\partial\chi}{\partial r}} - \frac{\frac{\partial\chi}{\partial\theta}}{\left(\frac{\partial\chi}{\partial r}\right)^2}\frac{\partial^2\chi}{\partial m^2} - \frac{\frac{\partial^2\chi}{\partial\theta^2}}{\frac{\partial\chi}{\partial\theta}}\right\} - \tan\beta\,(1 + \cos^2\beta) \qquad (4)$$

$$B = r \tan\beta \frac{\partial W}{\partial r} \tag{5}$$

and

$$\beta = \tan^{-1} \frac{W_\theta}{W_r} \tag{6}$$

In the first step of calculation, the mass flow through the guided vane nozzle is reduced sufficiently so that the flow is completely subsonic throughout the passage. The finite difference solution is obtained as mentioned before. In the second calculating step, the velocity distribution based on the actual mass flow is obtained by means of the velocity gradient equation (3) using the information obtained in the first calculating step.

DESCRIPTION OF THE GUIDE VANE NOZZLE

DATA USED IN THE CALCULATIONS:

The cases presented here are based on the following inlet conditions:

Inlet total temperature,	T_t	=	1110°K
Specific heat ratio,	γ	=	1.328
Speed of sound,	a	=	650 m/s
Gas constant,	R	=	287.4 J/Kg °K
Inlet average velocity,	V_{ave}	=	42 m/s
Mass flow per one vane,	w	=	0.0106 Kg/s
Inlet total pressure,	P_t	=	6.894×10^5 N/m^2

Two radial guide vane configurations are shown in Figures 5 and 6. Figure 7 shows the mean camber line for the two blade shapes under consideration. The coordinates of the two guide vane blades are given in Tables 1 and 2. The five different

nozzle axial width configurations which are shown in Figure 8 were investigated. The input data for the program are given in Table 3.

COMPUTER RESULTS AND DISCUSSIONS

The analytical results obtained for the two guide vane blade configurations are presented in Figures 9 through 19. The blade surface velocity distributions are shown in Figures 9 and 10. Both configurations result in the same tendencies in velocity variations on the blade surfaces. A large velocity gradient exists near the leading edge of the blade concaved surface, for configuration 2. This may be attributed to its larger leading edge radius. The streamline patterns of the flow in the vane nozzles are shown in Figures 11 and 12. Identical flow patterns are obtained in both cases. The blade surface temperature distributions are presented in Figures 13 and 14. The changes in the gas flow temperature are small since the mass flow considered here is less than the vane critical mass flow. It may be noted from the velocity and the temperature distributions that the differences in the flow parameters between the concave surface and the convex surface are more pronounced for configuration 2 than for configuration 1. Consequently, configuration 1 is preferable for guide vanes of radial turbines. Figure 15 shows the circumferential variation in the velocity at the guide vane leading edge for three different nozzle entrance lengths. Very small differences are observed for the entrance lengths between a half and one times the radial blade chord. Figure 16 shows the effect of the guide blade shape on the velocity profile at the entrance between two successive blade leading edges. The variation in the flow direction, α, for the two blade configurations, is given in Figure 17. The variation of the radial and tangential velocity components at the vane entrance are shown in Figures 18 and 19 for the two blade configurations considered. It is noted that unlike

the radial component, the tangential velocity component has a symmetric distribution between two successive blades. The mass flow rate at the guide vane inlet varies considerably in the circumferential direction. The tendency is such that the mass flux is greater at the blade concave surface than that at the convex surface.

From Figures 9 and 10, some features of the flow behavior over a blade in a radial cascade can be observed. It is noticed that the pressure is lower on the blade surface with the concave shape, and higher on the convex surface. This is the opposite of what is expected in an axial cascade where the convex surface is the suction side and the concave surface is the pressure side. This theoretical result was confirmed experimentally in our laboratory for the blade curvature settings similar to those investigated analytically. The blade curvature setting is reversed, however, in recent guide vane designs.

Figures 20 and 21 show the effect of the channel axial width variation on the inlet velocity profiles. The channel configurations were shown in Figure 8. It was found that by changing the channel width in the entrance region, very little change in the inlet profiles was noticed. On the other hand, changing the channel width inside the blade region resulted in considerable changes in the velocity profiles, as can be seen in Figures 20 and 21.

CONCLUSIONS

The three-dimensional flow behavior existing in the scroll will effect the mass flow distribution through the guide vanes. From this study, it is found that the blade shape effects the inlet velocity profiles, causing a variation in the flow mass flux at the guide vane inlet. The channel width in the guide vane entrance region does not influence the inlet velocity profiles.

REFERENCES

1. Wood, Homer T., "Current Technology of Radial Inflow Turbines for Compressible Fluids," Transactions of the ASME, January 1963, pp. 72-83.
2. Barnard, M.C.S. and Benson, R.S., "Radial Gas Turbines," The Institute of Mechanical Engineers, Warwick, April 1969.
3. Von der Nuell, W.T., "Single Stage Radial Turbines for Gaseous Substances with High Relative and Specific Speed," Transactions of the ASME, 1952, p. 499.
4. Hawthorne, W.R., "Secondary Circulation in Fluid Flow," Proceedings of Royal Society, Vol. 206, 1951, pp. 374-386.
5. Squire, H.B. and Winter, K.G., "The Secondary Flow in a Cascade of Aerofoils in a Non-Uniform Stream," Journal of Aeronautical Sciences, Vol. 18, 1951, pp. 271-274.
6. Katsanis, Theodore, "Fortran Program for Calculating Transonic Velocities on a Blade to Blade Stream Surface of a Turbomachine," NASA TN-D 5427, September 1969.

LIST OF SYMBOLS

a	Speed of sound, m/s (ft/sec)
C_r	Radial chord
b	Stream Channel thickness normal tc meridional streamline
ℓ	Entrance region length
P	Pressure, N/m^2 (psia)
R	Gas constant, J/Kg °K (ft-lb/lb °F)
r	Radial coordinate
T	Temperature, °K (°R)
V	Fluid velocity, m/s (ft/sec)
w	Nozzle vane mass flow, Kg/s (lb/sec)
W	Velocity, m/s (ft/sec)
α	Angle between radial and velocity directions
β	Angle between rel. velocity vector and meridional plane, radians
γ	Specific heat ratio
θ	Angular coordinate, radians
ρ	Density, Kg/m^3 ($slug/ft^3$)
χ	Stream function

Subscripts

r	Radial component
t	Total or stagnation conditions
θ	Tangential component

$r - r_i$ (mm)	θ	
	UPPER SURFACE (degrees)	LOWER SURFACE (degrees)
2.54	4.20	- 0.15
5.71	9.05	5.50
8.25	13.07	10.43
10.80	17.35	14.95
13.33	22.22	19.50
15.87	27.35	24.75
17.14	30.00	27.60
18.41	33.05	30.65

TABLE 1 - BLADE COORDINATES

FOR CONFIGURATION 1

$r - r_i$ (mm)	θ	
	UPPER SURFACE (degrees)	LOWER SURFACE (degrees)
2.54	3.95	--
5.71	8.70	1.20
8.25	12.71	5.85
10.80	16.90	11.85
13.33	21.85	16.62
15.87	26.97	23.00
17.14	30.00	26.55
18.41	33.05	30.65

TABLE 2 - BLADE COORDINATES

FOR CONFIGURATION 2

TABLE 3 - INPUT DATA FOR RADIAL GUIDE VANE*

```
TSONIC  RADIAL STATOR CONSTANT X-SECTION
      GAM              AR              TIP             RHOIP           WTFL                            OMEGA           DRF
    1.328000        1718.000        2000.000       0.42200000-02  0.30000000-02   0.0             0.0             1.827813
     BETAI           BETAO           CHORDF          STGRF
    45.00000        73.50000       0.64830000-01    0.5900050
     REDFAC          DENTOL
   0.5000000       0.10000000-01
  MBI  MBO          MM  NBBI  NBL NRSP
  17   37    0    0   47   15   13
    BLADE SURFACE 1  --  UPPER SURFACE
      RI1             RO1             BETI1           BETO1           SPLNO1
  0.67883000-02   0.13028000-02     60.00000        78.50000        10.00000
     MSP1  ARRAY
  0.0             0.83300000-02   0.18750000-01   0.27083000-01   0.35416000-01   0.43750000-01   0.52083000-01   0.56250000-01
  0.60416000-01   0.0
     THSP1  ARRAY
  0.0             0.69000000-01   0.1518000       0.2220500       0.2952000       0.3820000       0.4707000       0.5226000
  0.5768000       0.0
    BLADE SURFACE 2  --  LOWER SURFACE
      RI2             RO2             BETI2           BETO2           SPLNO2
  0.67803000-02   0.13028000-02     30.00000        71.50000        9.000000
     MSP2  ARRAY
  0.0             0.18750000-01   0.27083000-01   0.35416000-01   0.43750000-01   0.52083000-01   0.56250000-01   0.60416000-01
  0.0
     THSP2  ARRAY
  0.0             0.21960000-01   0.1021490       0.1973000       0.2900000       0.4020000       0.4648000       0.5250000
  0.0
     MR  ARRAY
 -0.50000000-01  -0.30000000-01  -0.15000000-01   0.0             0.83300000-02   0.18750000-01   0.27083000-01   0.35416000-01
  0.43750000-01   0.52083000-01   0.56250000-01   0.60416000-01   0.64830000-01   0.64083000-01
     RMSP  ARRAY
  0.3273000       0.3073000       0.2953000       0.2773000       0.2689000       0.2586000       0.2502500       0.2419200
  0.2336000       0.2252500       0.2210800       0.2169200       0.2132500       0.1849400
     BESP  ARRAY
  0.35200000-01   0.45200000-01   0.40000000-01   0.32917000-01   0.32917000-01   0.32917000-01   0.32917000-01   0.32910000-01
  0.32917000-01   0.32917000-01   0.32917000-01   0.32917000-01   0.32917000-01   0.32917000-01
   BLDAT  AANDK  ERSOR  STRFN  SLCRD  INTVL  SURVL
     1      1      0      1      2      3      2
```

* The input data is in English units.

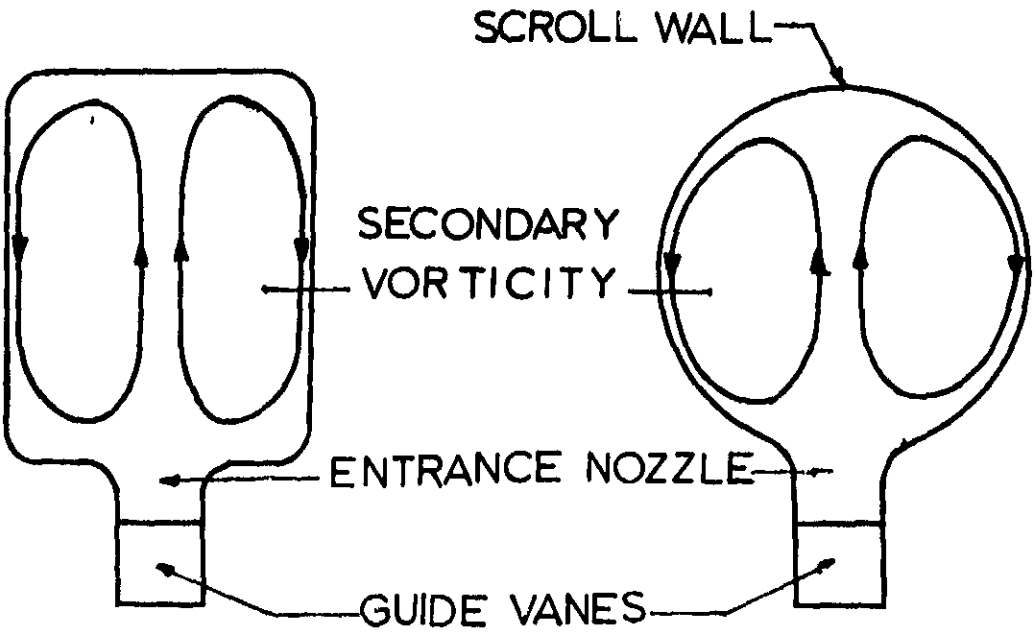

SCROLL CROSS SECTION

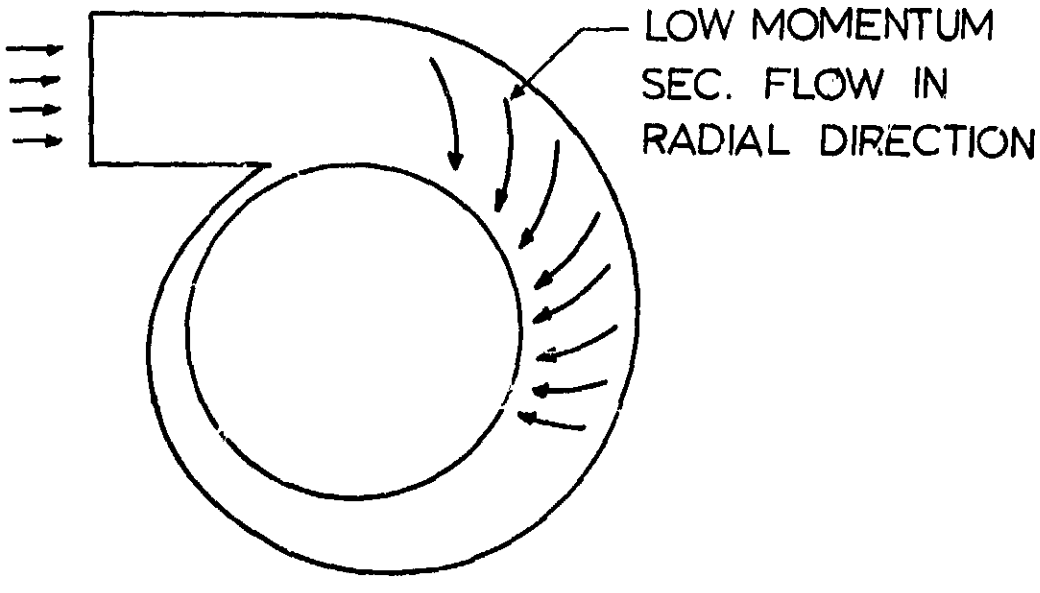

SCROLL FRONT VIEW

FIG. 1 SECONDARY FLOW IN SCROLLS

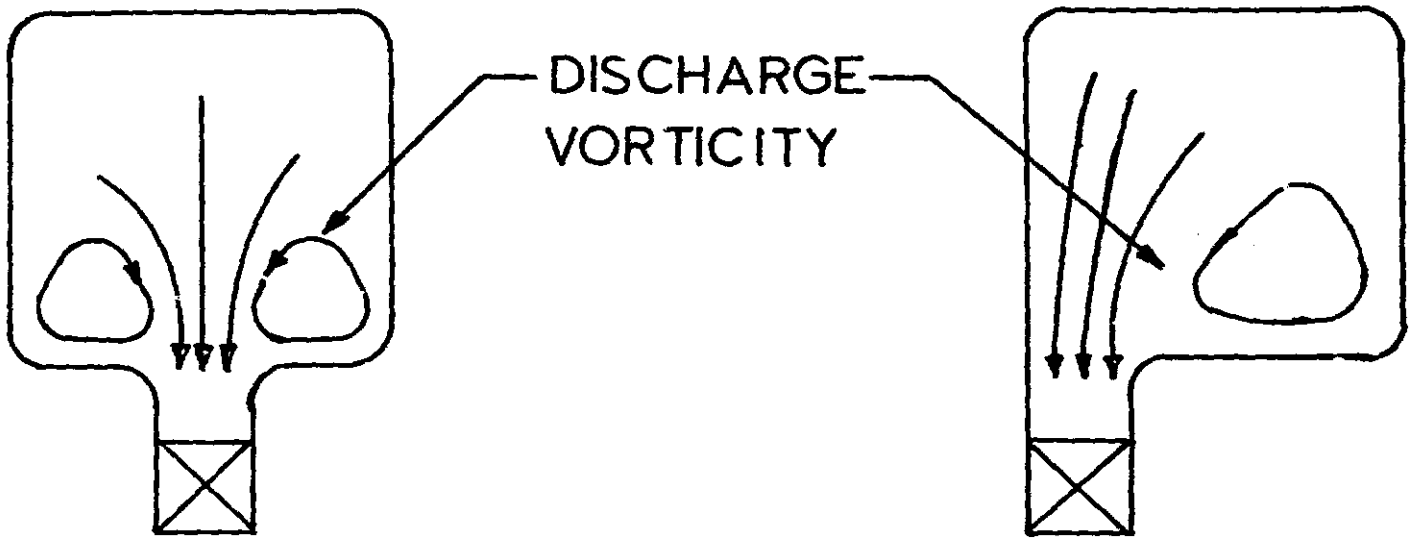

(a) MIDDLE ENTRANCE VANE (b) SIDE ENTRANCE VANE

FIG. 2 DISCHARGE VORTICITY

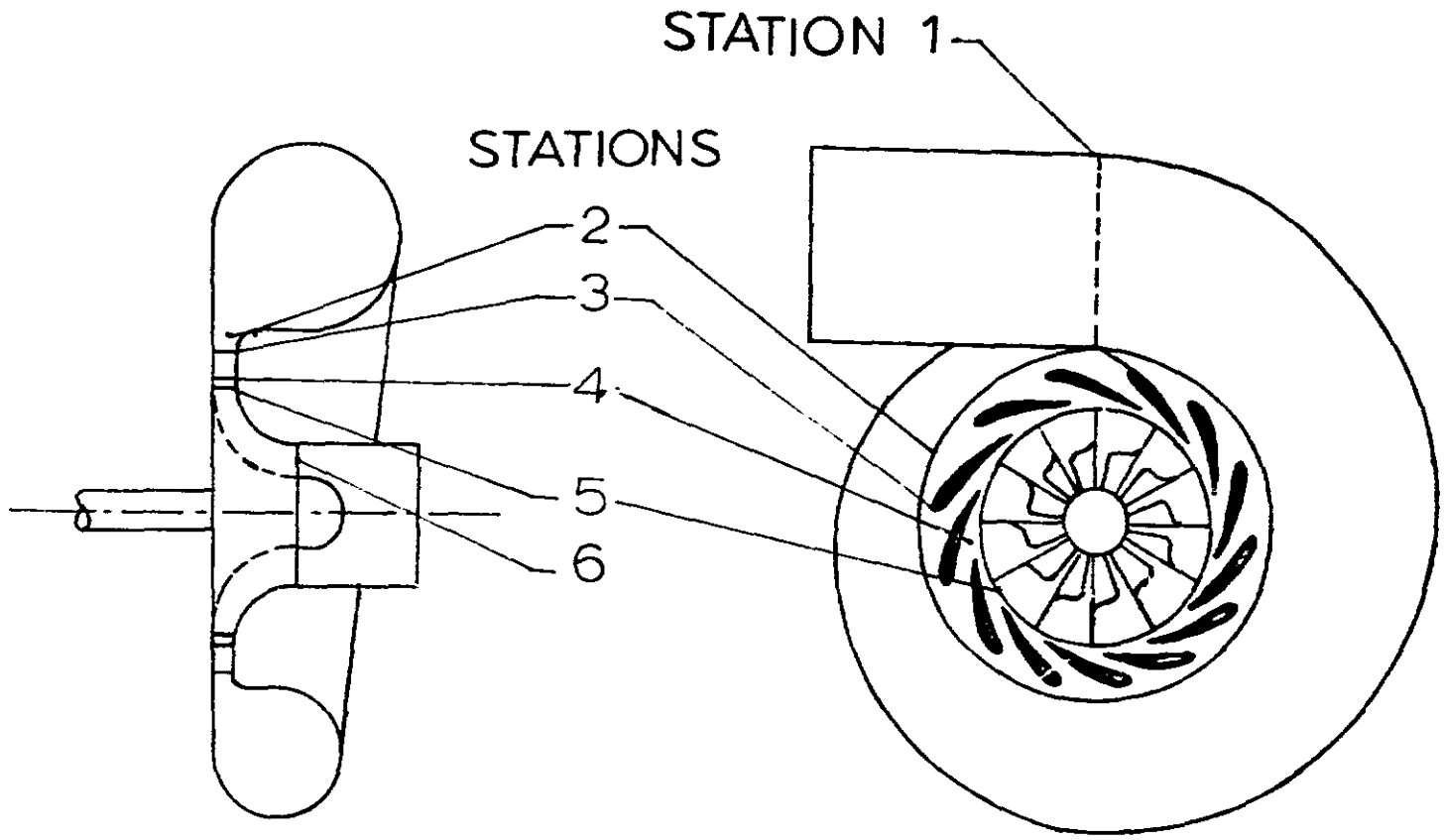

FIG. 3 SCHEMATIC OF TYPICAL RADIAL TURBINE

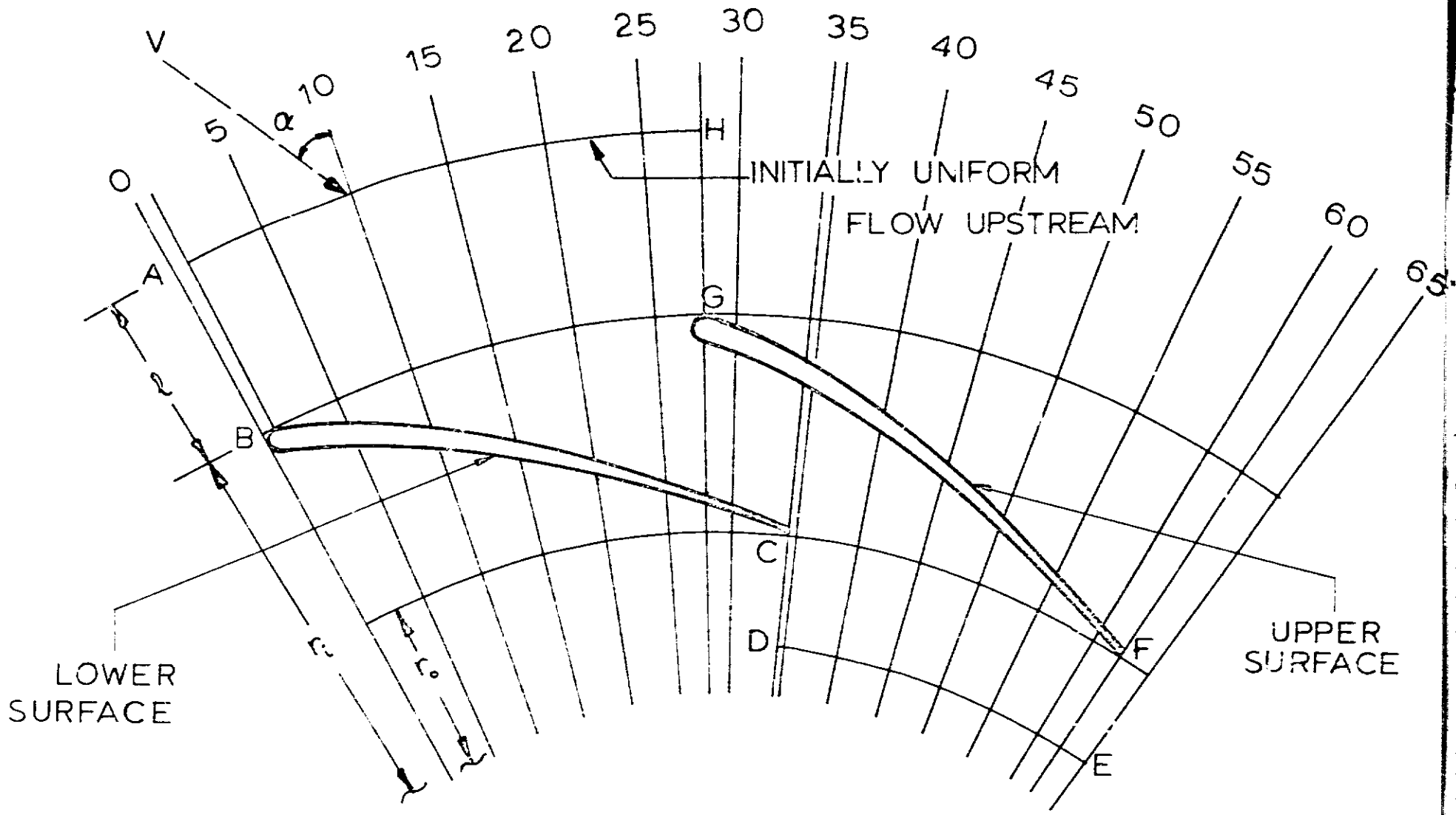

FIG. 4 GUIDE VANE BLADE TO BLADE REGION

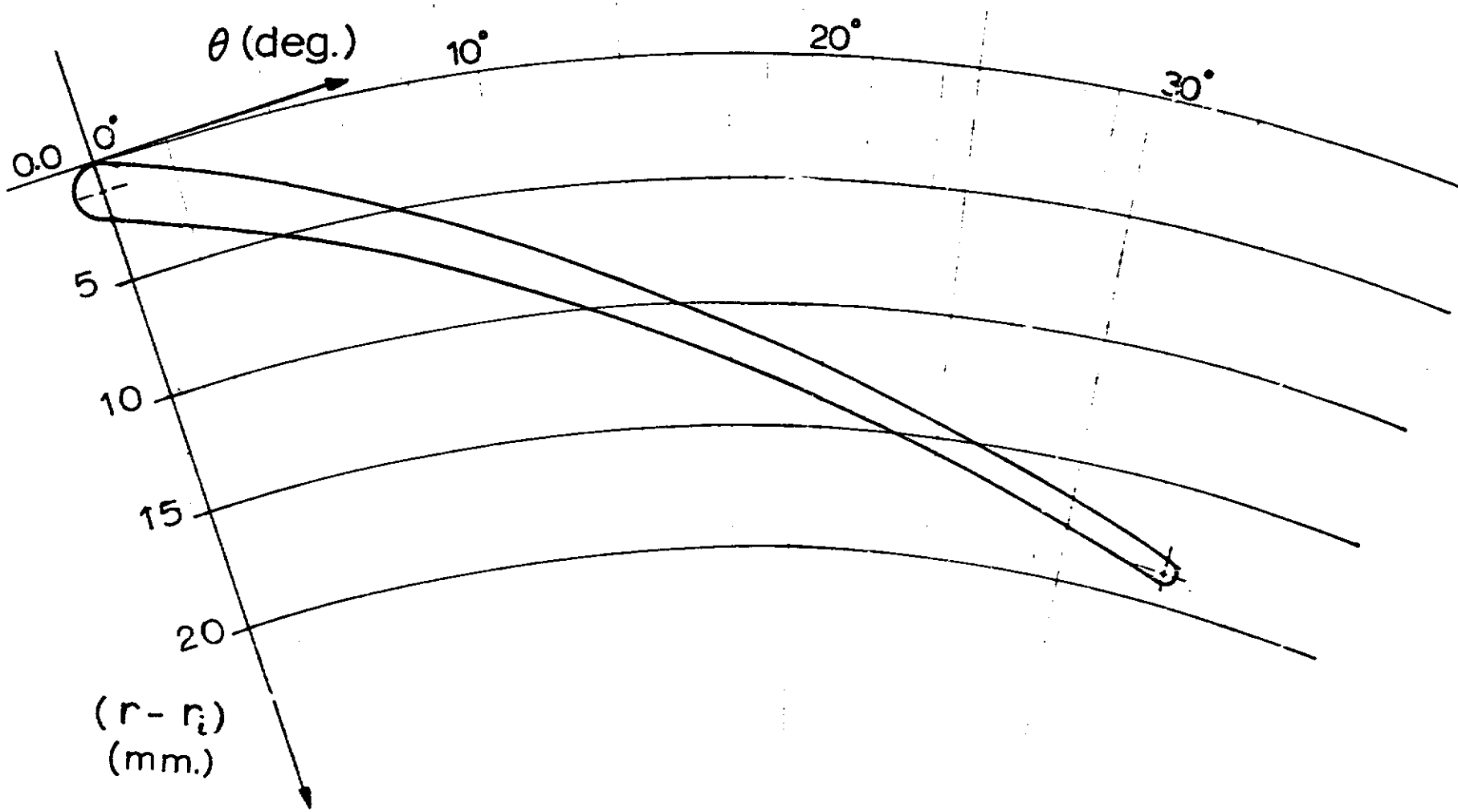

FIG. 5 BLADE CONFIGURATION 1

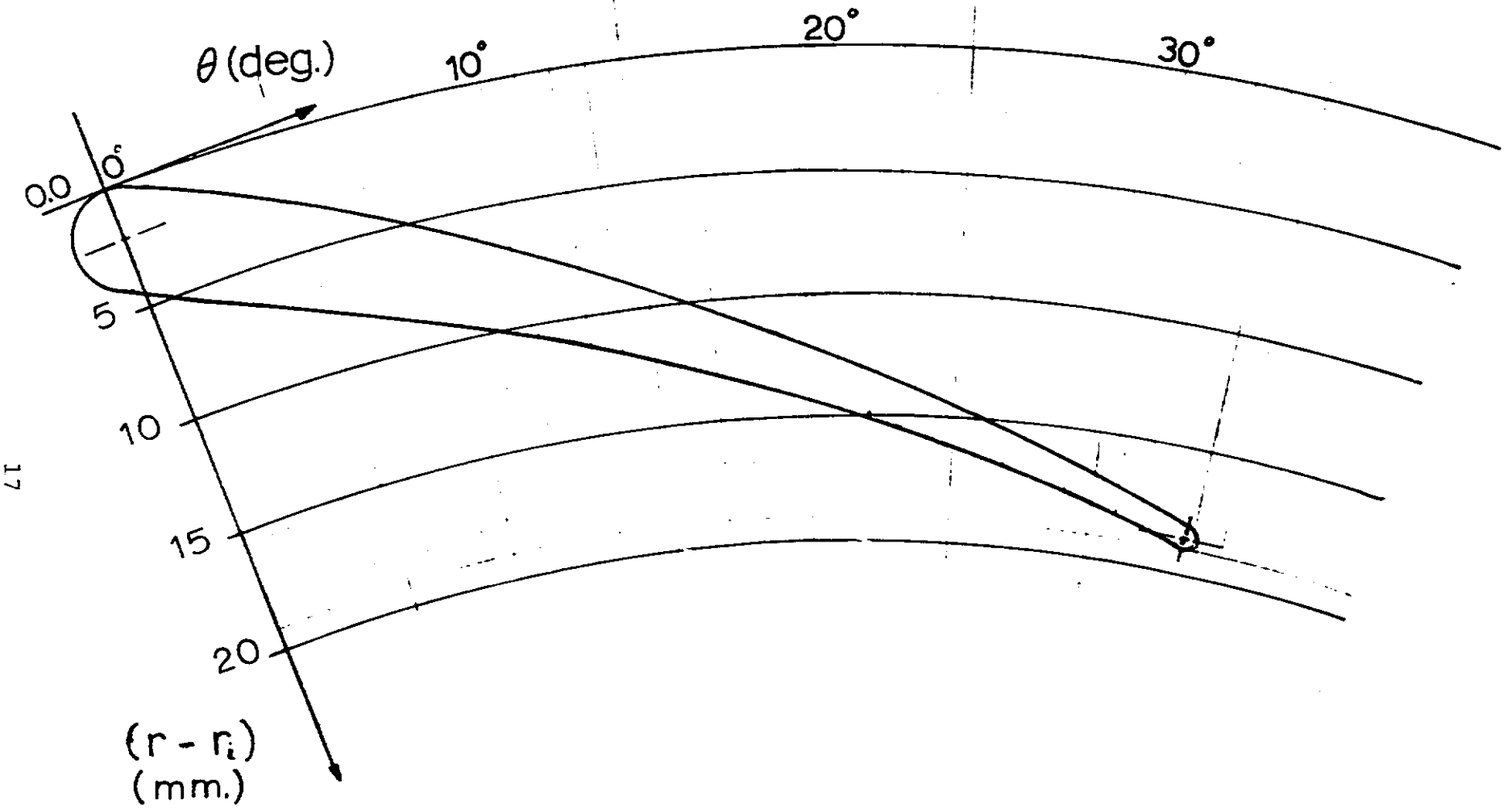

FIG. 6 BLADE CONFIGURATION 2

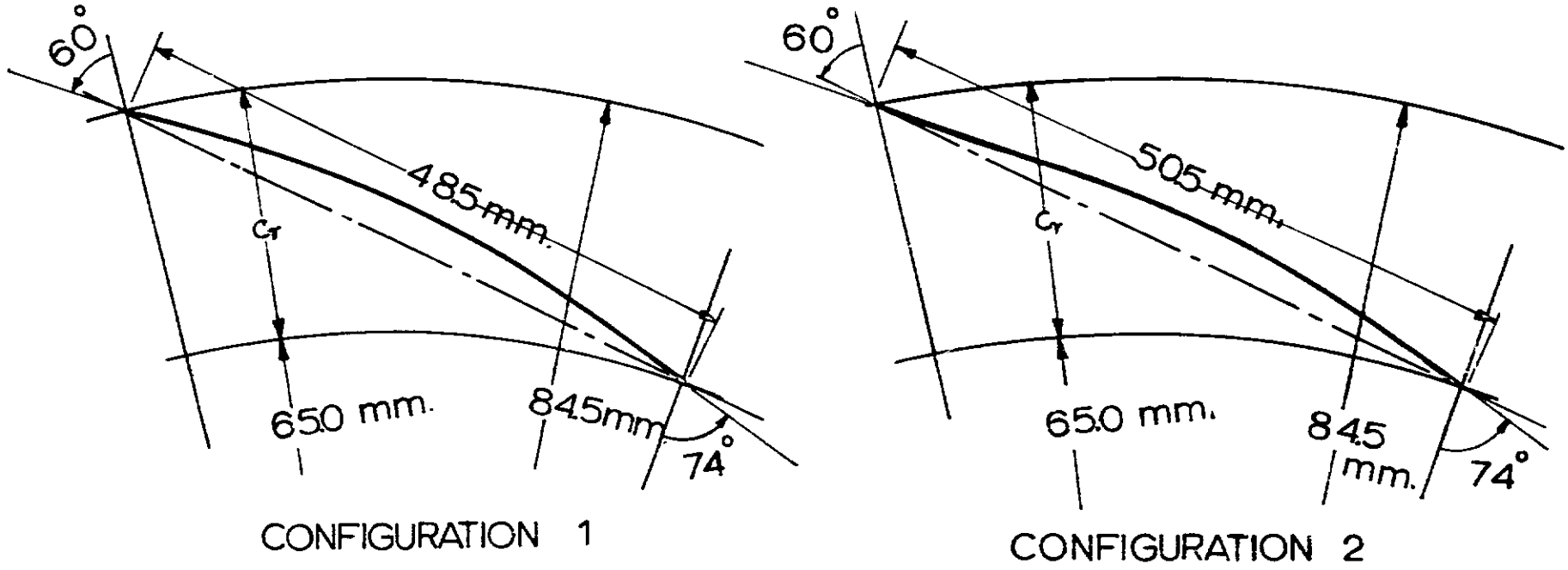

FIG. 7 BLADE MEAN CAMBER LINE CONFIGURATIONS

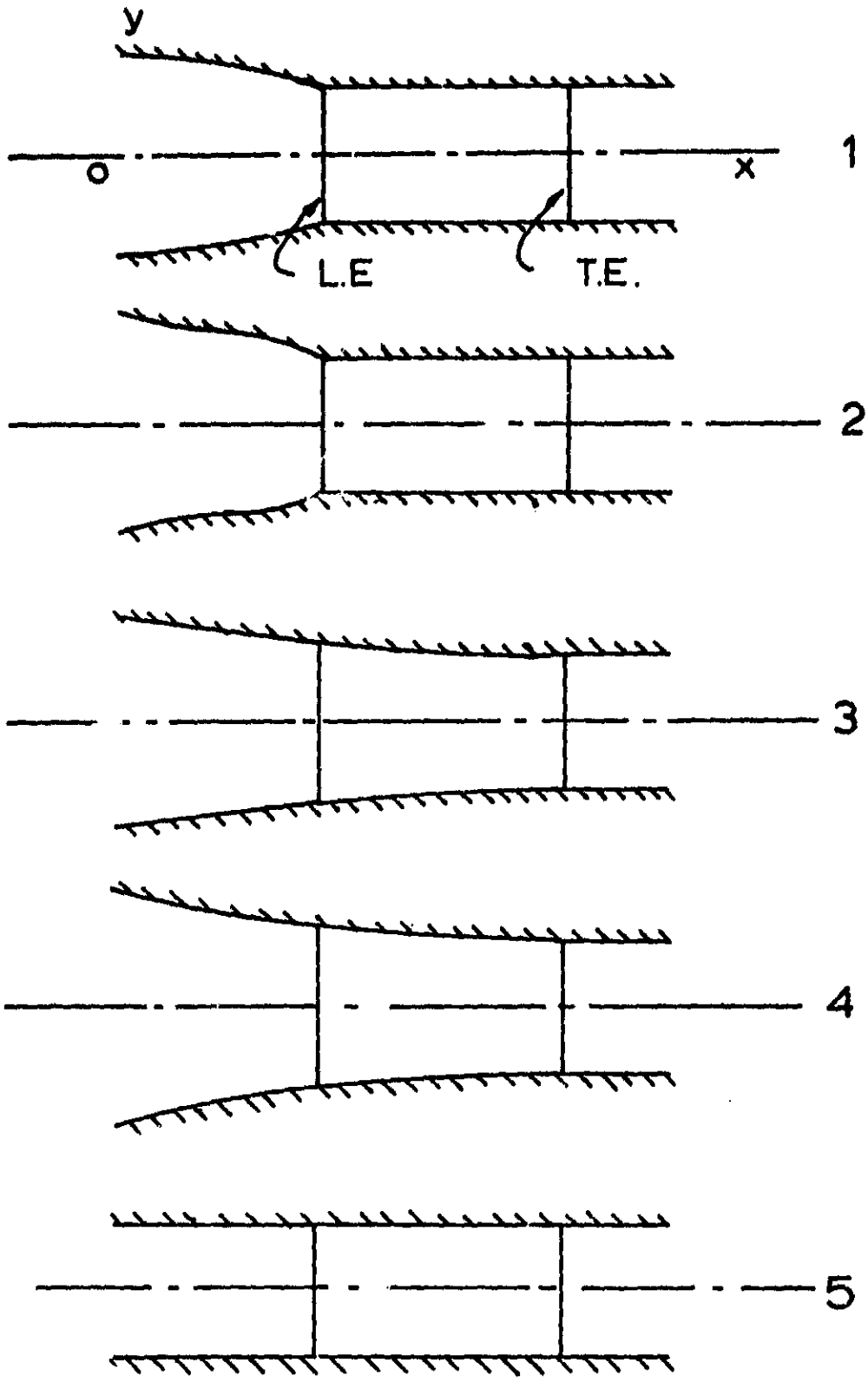

FIG. 8 VARIOUS CHANNEL WIDTH CONFIGURATIONS

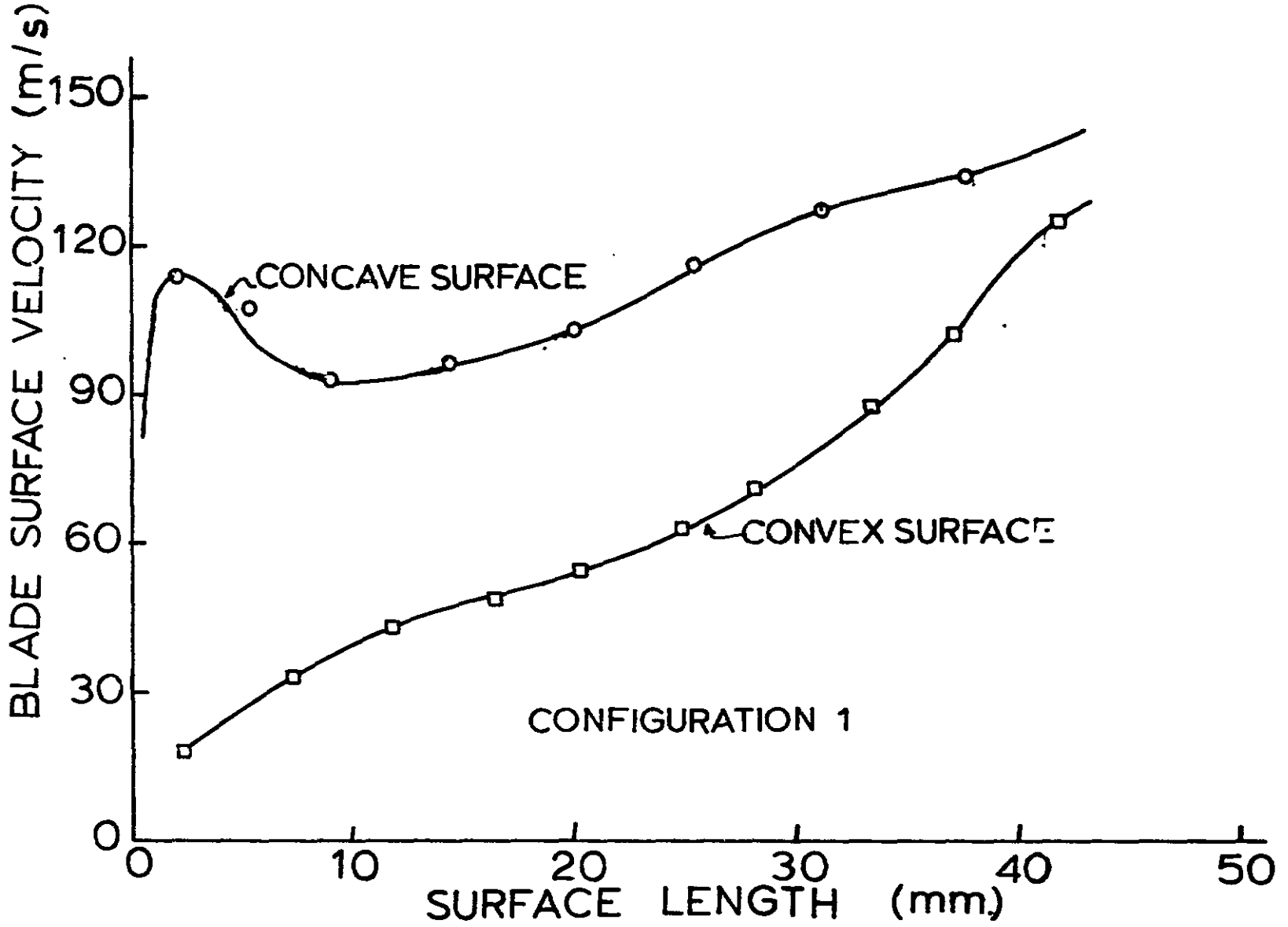

FIG. 9 BLADE SURFACE VELOCITY VS. SURFACE LENGTH

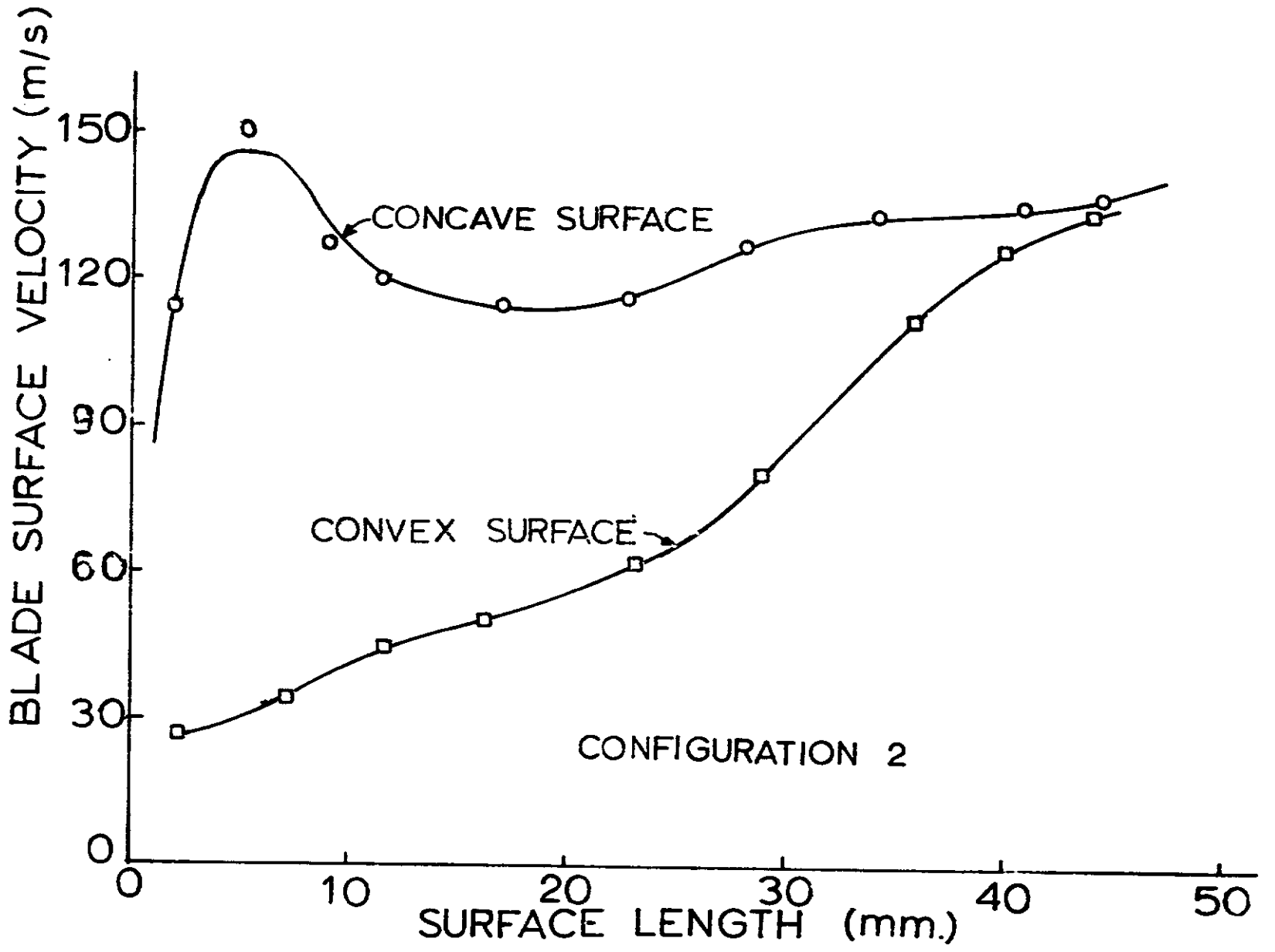

FIG.10 BLADE SURFACE VELOCITY VS. SURFACE LENGTH

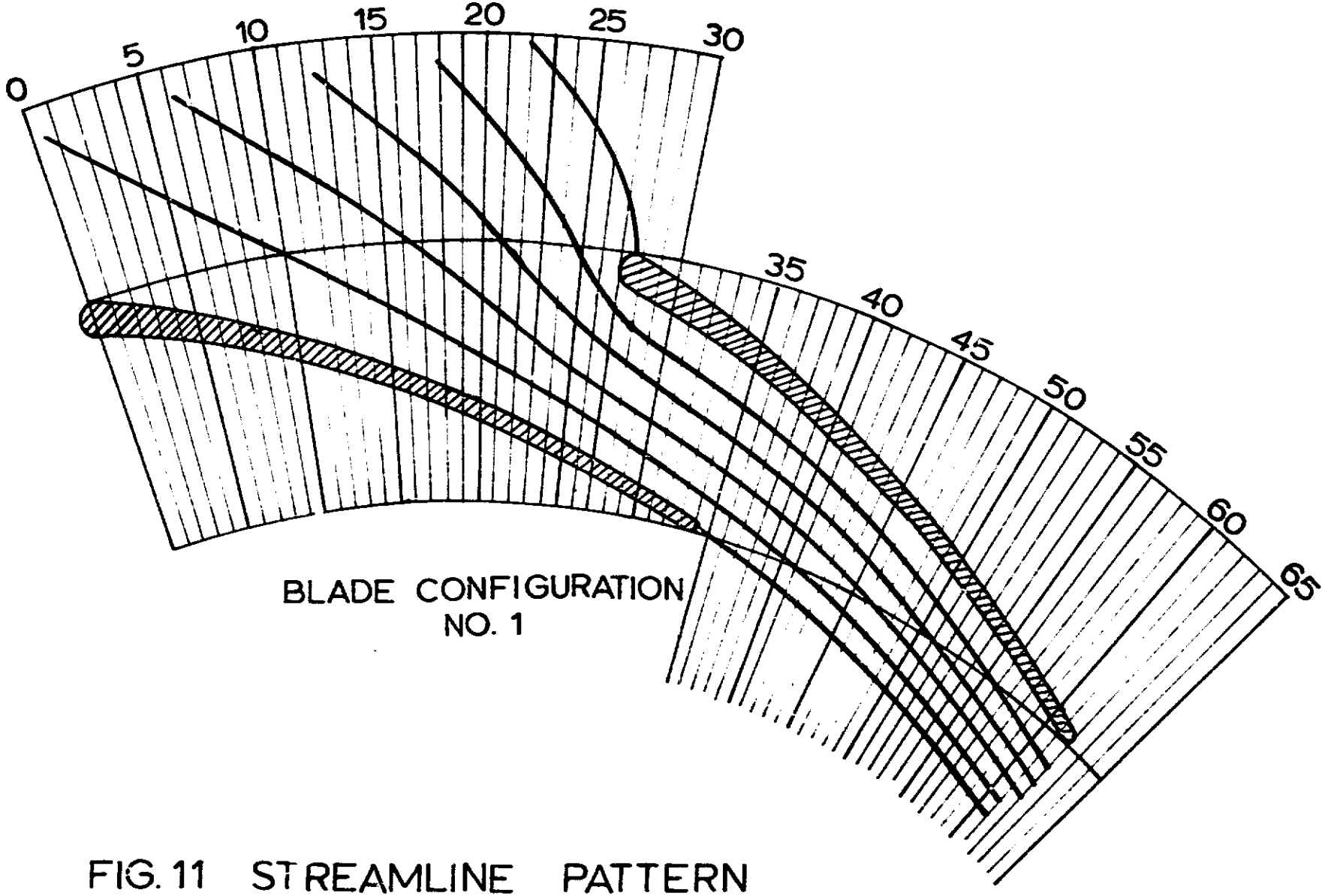

FIG. 11 STREAMLINE PATTERN

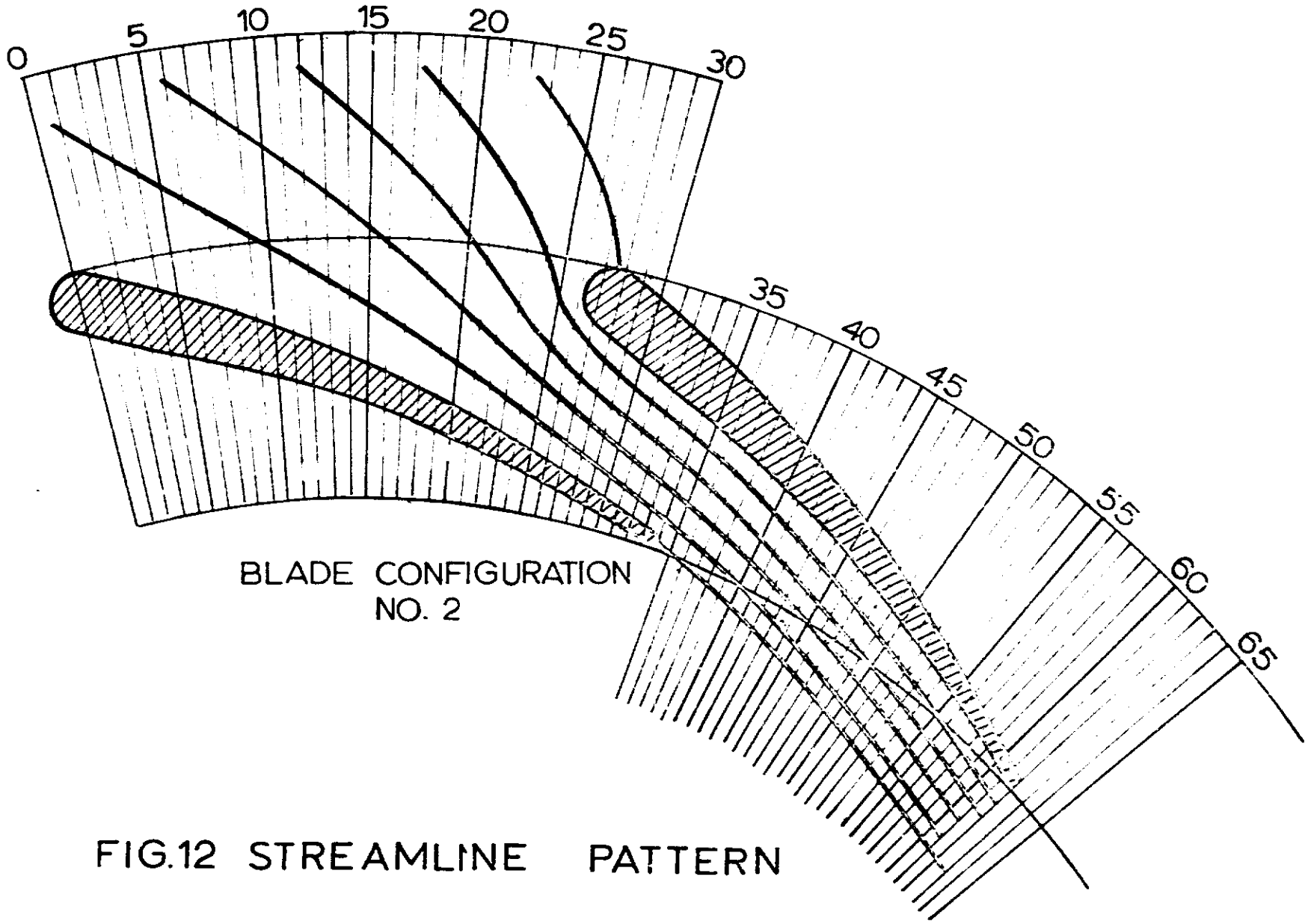

FIG.12 STREAMLINE PATTERN

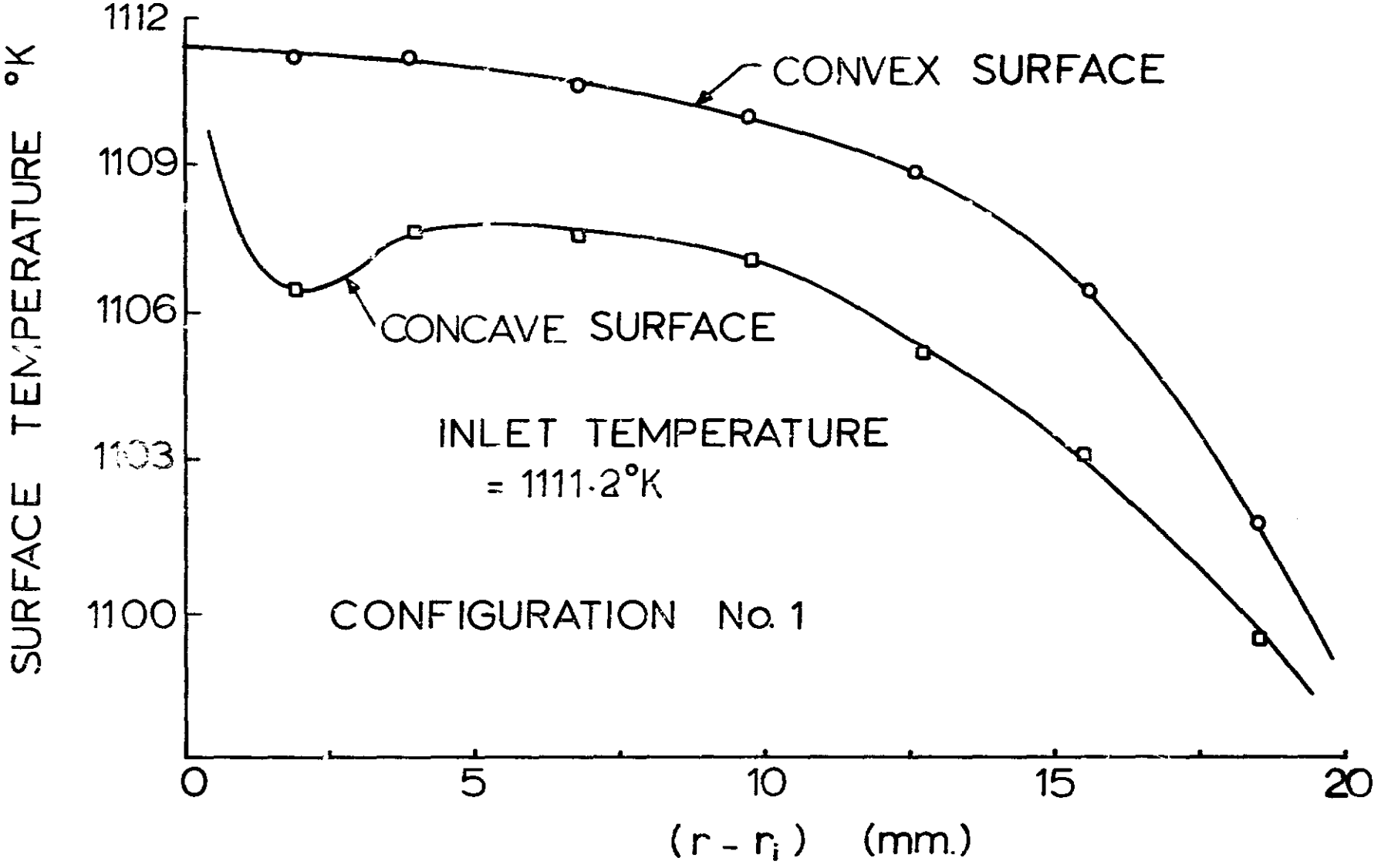

FIG.13 SURFACE TEMPERATURE DISTRIBUTION

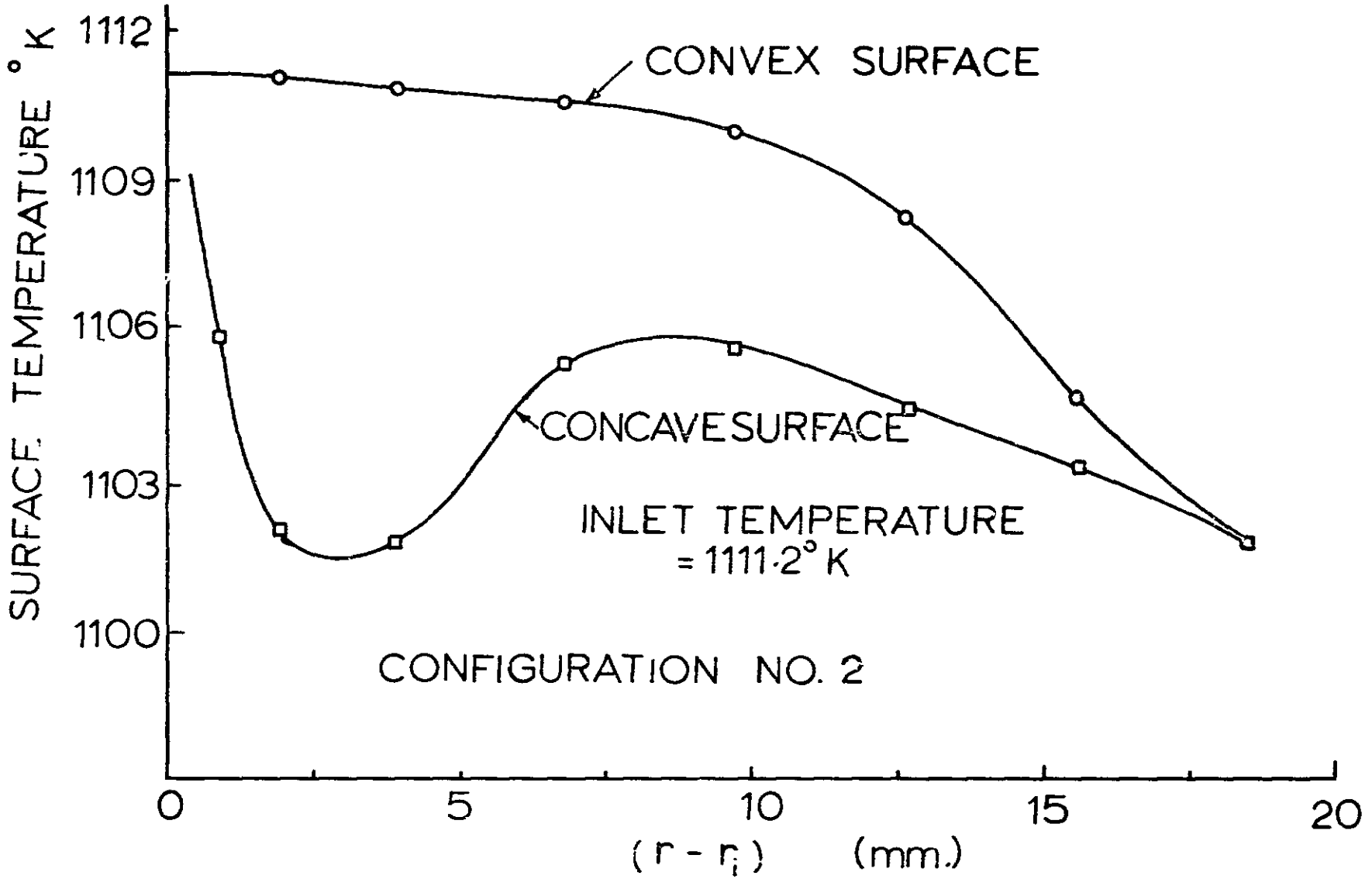

FIG. 14 SURFACE TEMPERATURE DISTRIBUTION

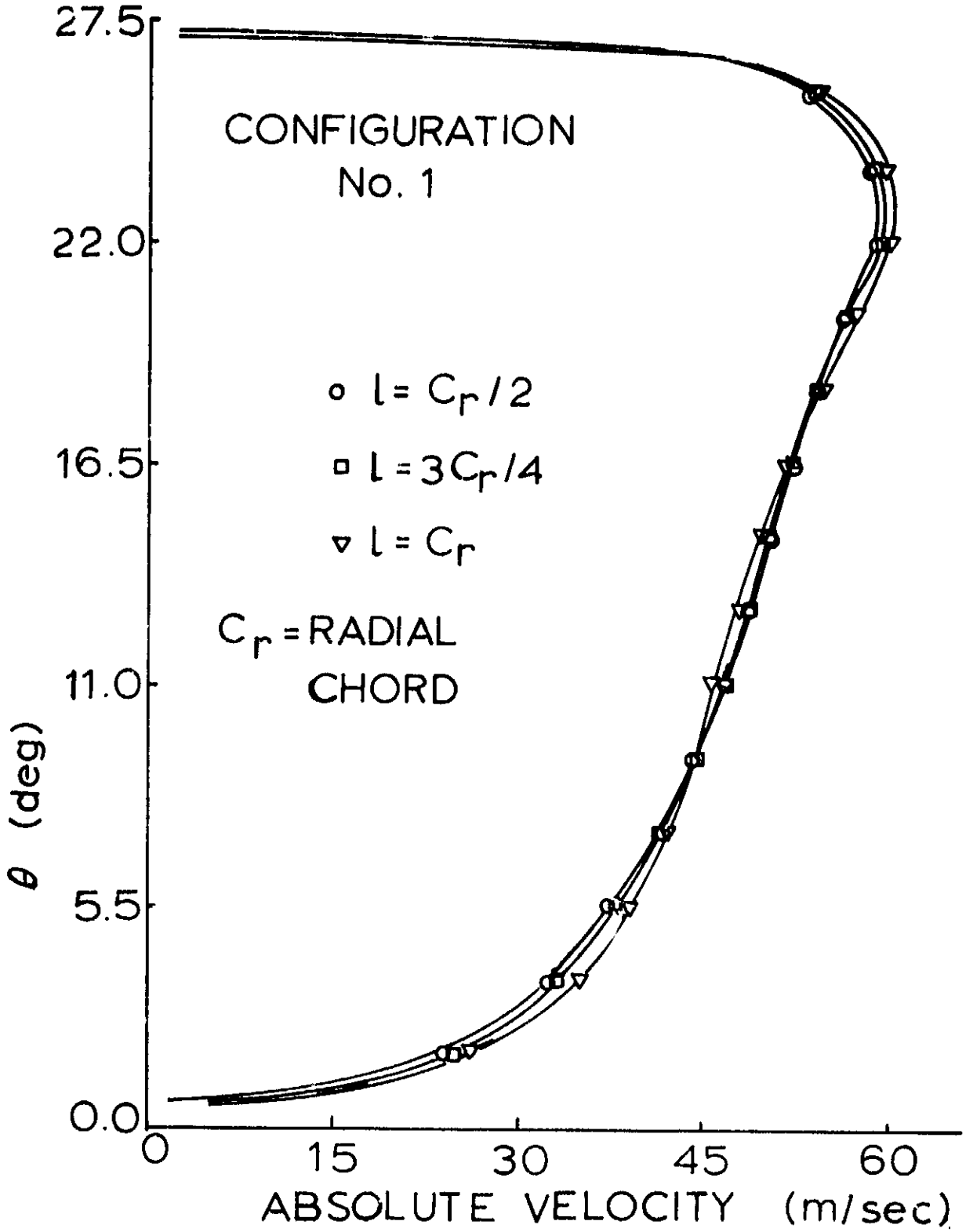

FIG.15 VELOCITY PROFILE AT VANE LEADING EDGE

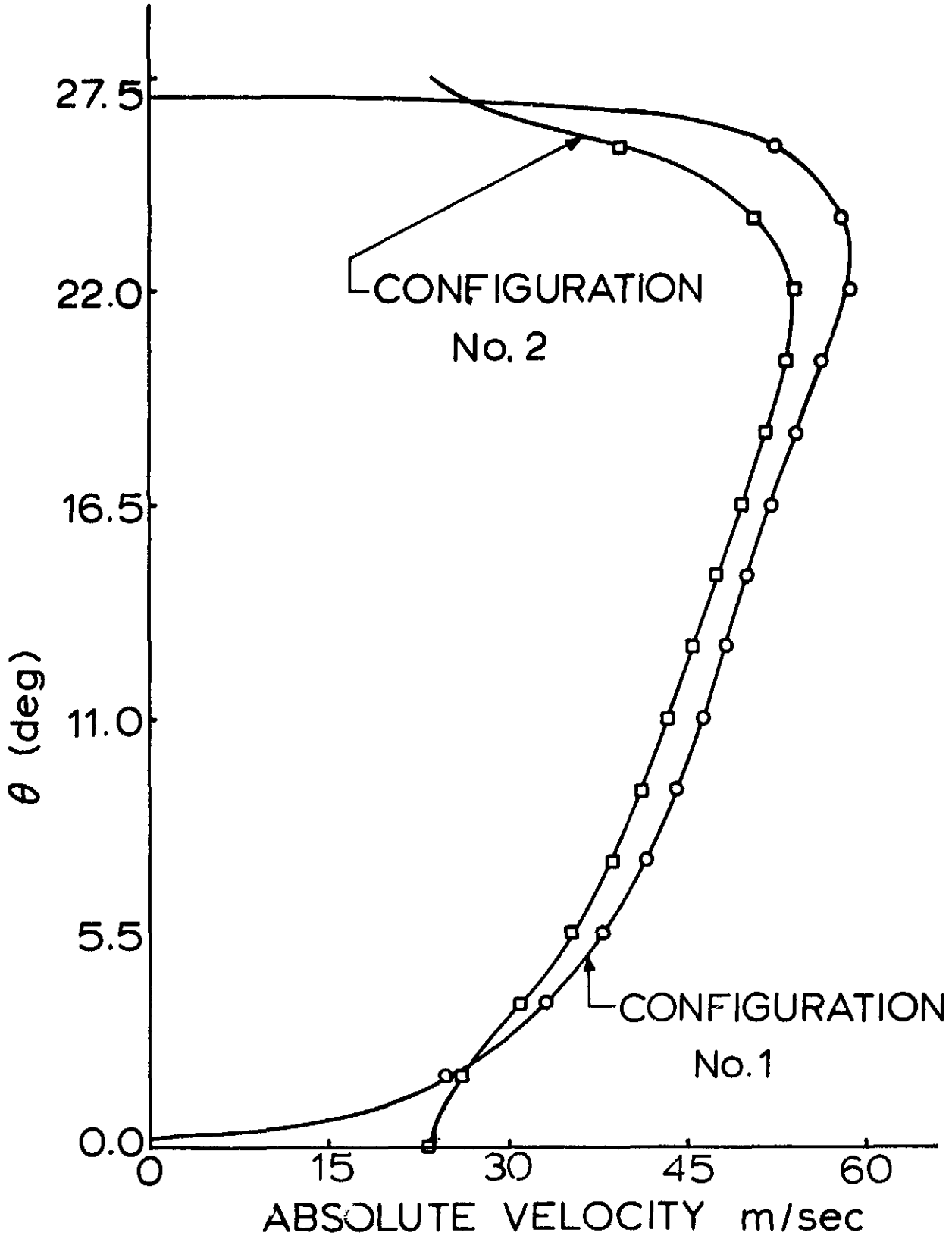

FIG.16 EFFECT OF BLADE SHAPE ON VEL. PROFILE AT VANE LEADING EDGE

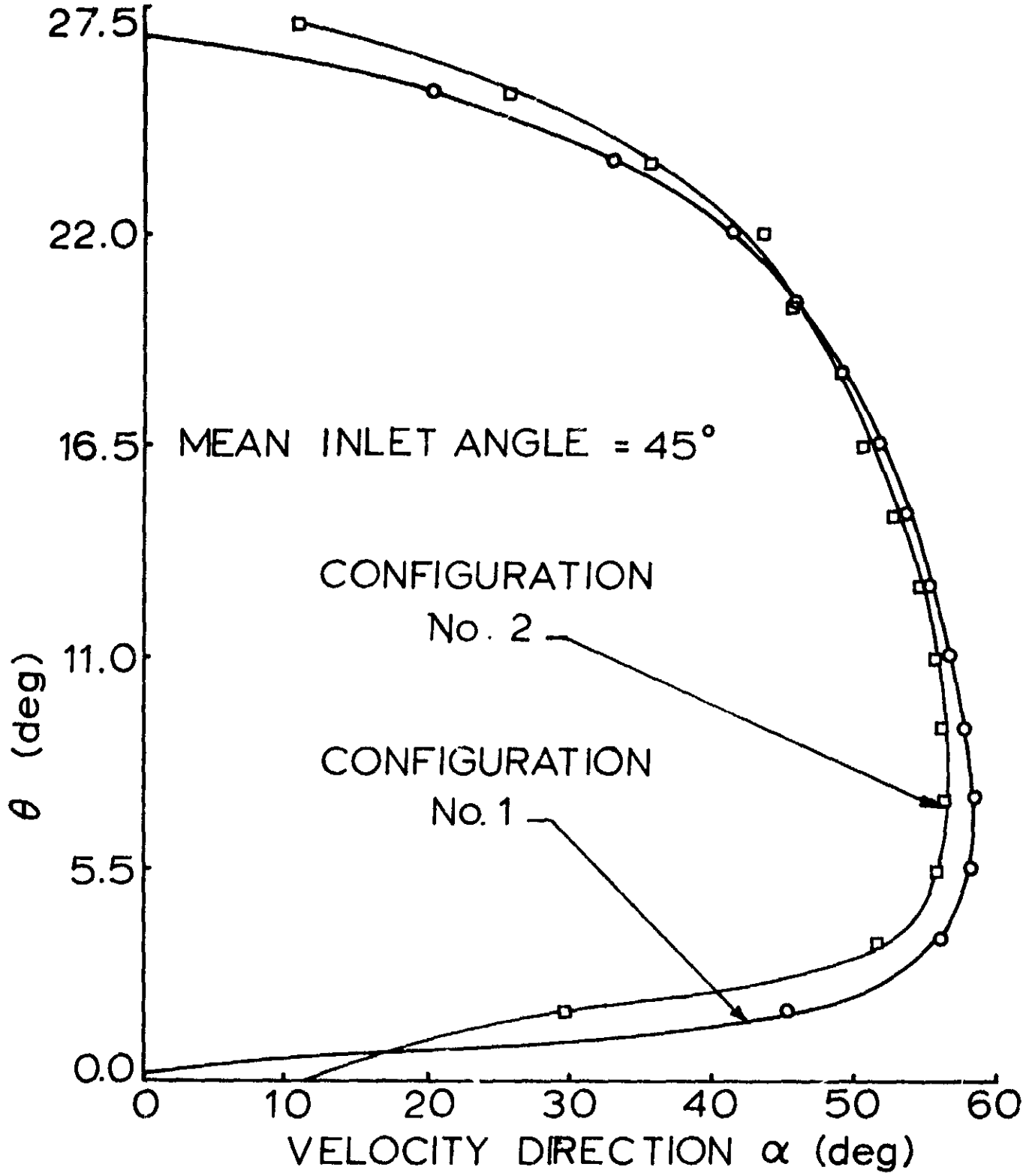

FIG.17 VARIATION OF VELOCITY DIRECTION AT GUIDE VANE LEADING EDGE

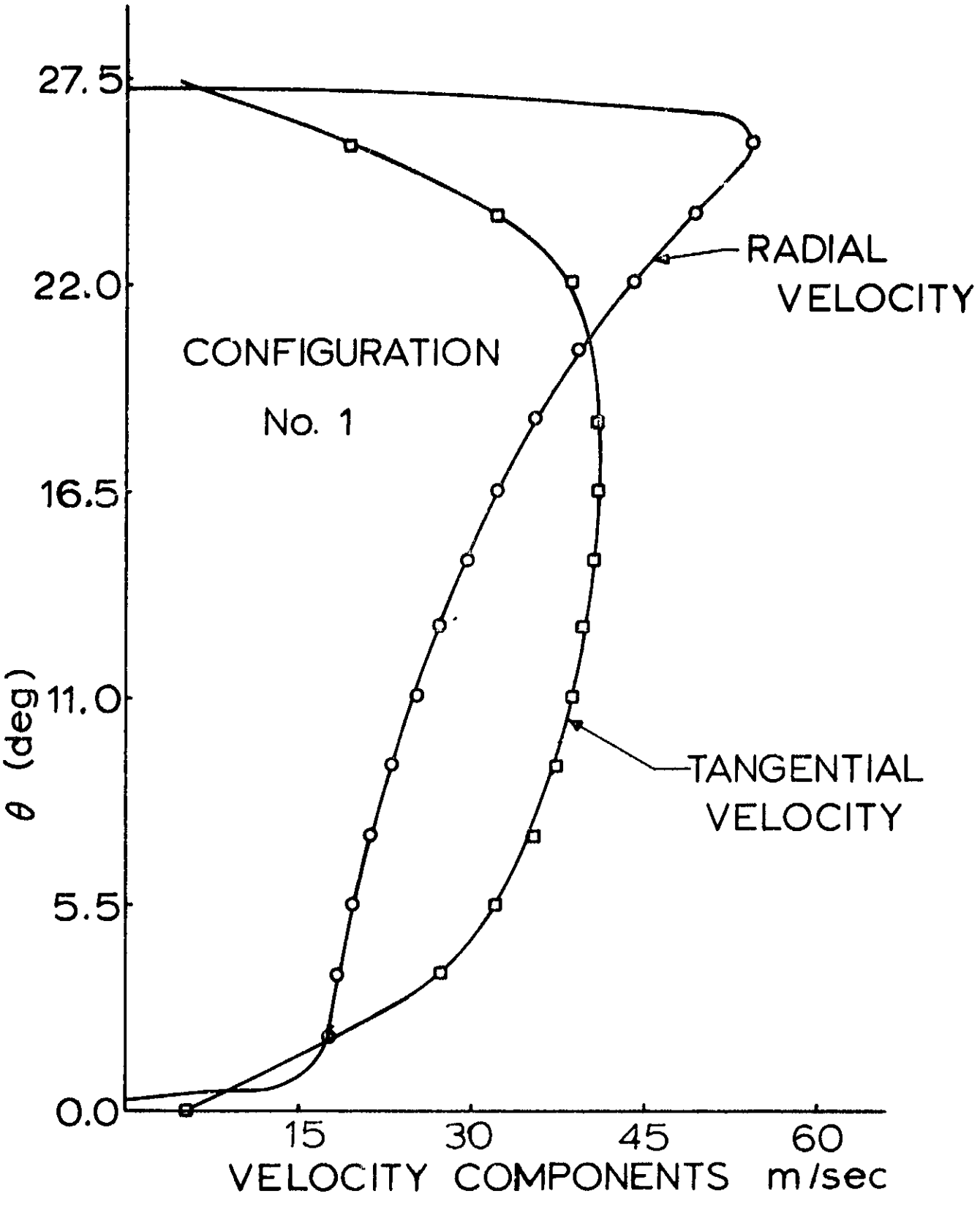

FIG. 18 VELOCITY COMPONENTS AT INLET

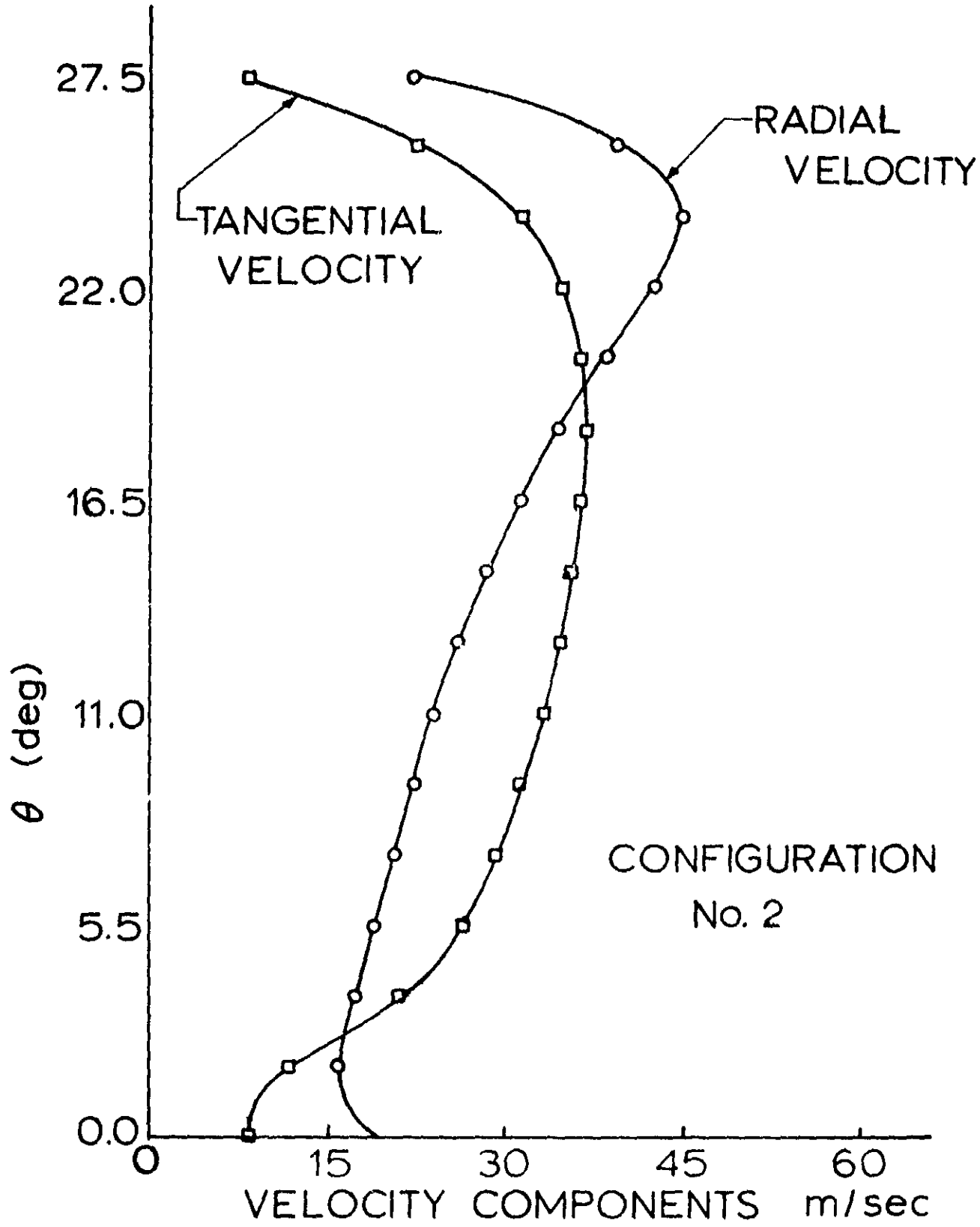

FIG. 19 VELOCITY COMPONENTS AT INLET

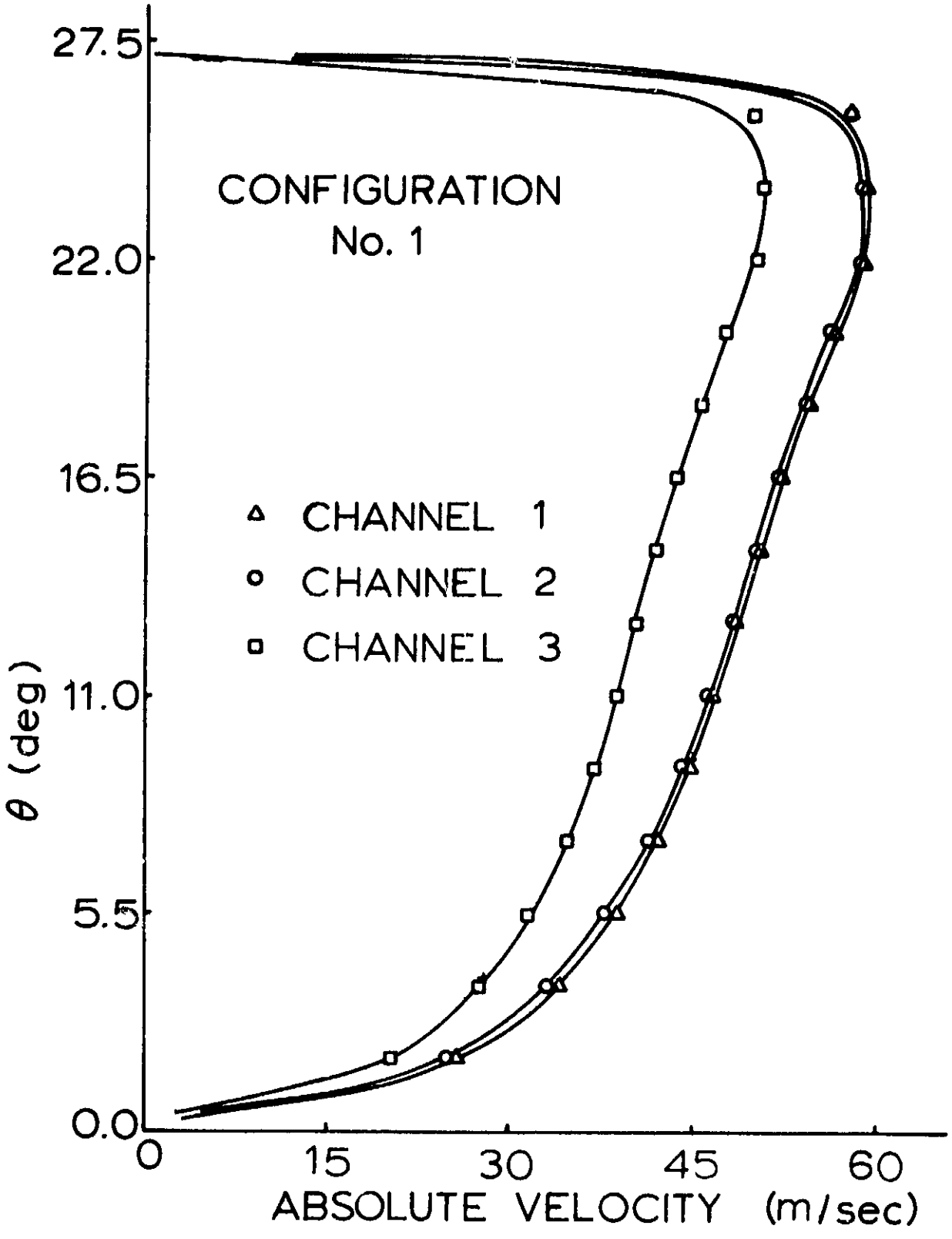

FIG. 20 INLET PROFILES: EFFECT OF CHANNEL VARIATION

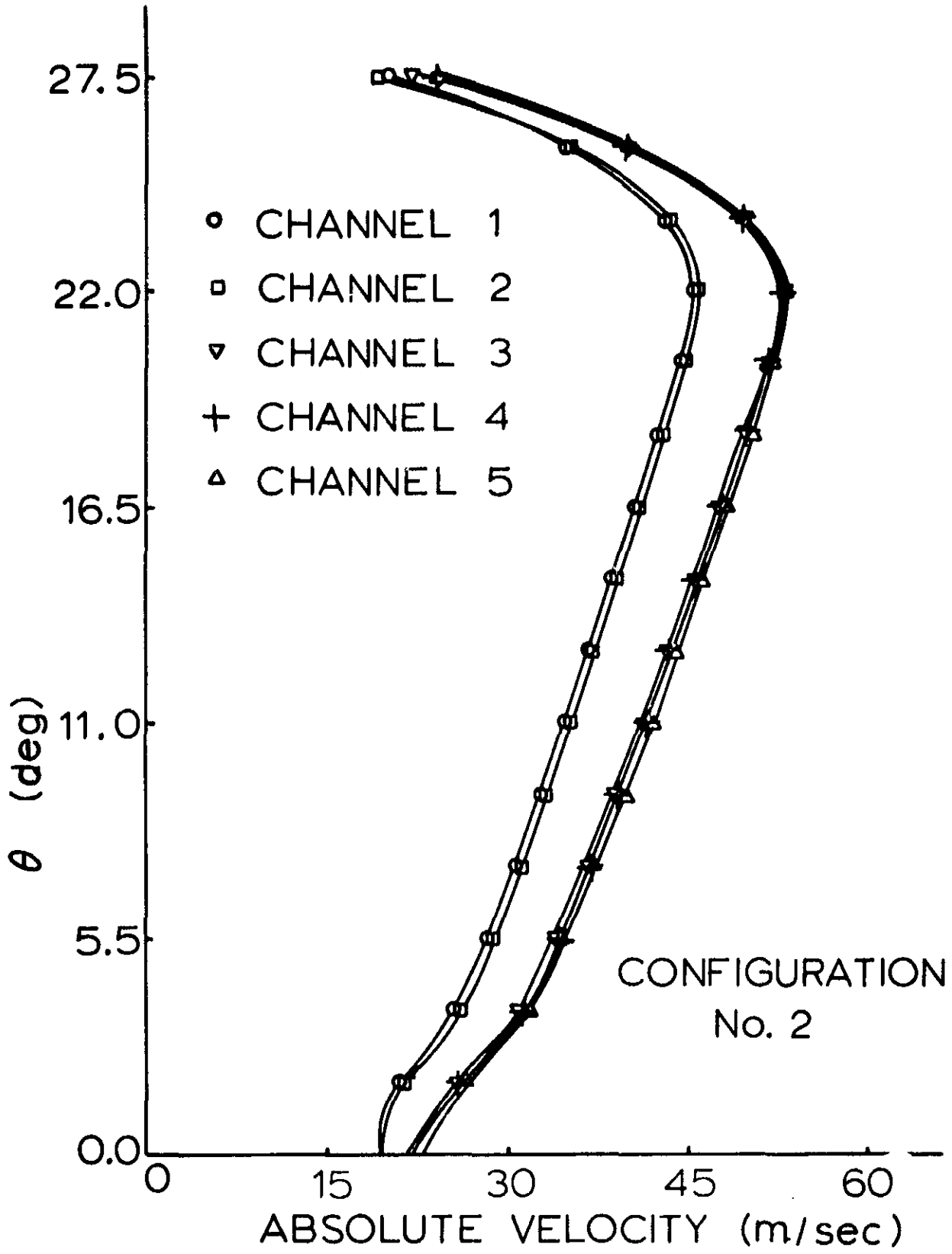

FIG.21 INLET PROFILES: EFFECT OF CHANNEL WIDTH